SECOND EUROPEAN CONFERENCE ON EARTHQUAKE ENGINEERING
AND SEISMOLOGY, ISTANBUL AUG. 25-29, 2014

CYCLIC PERFORMANCE OF RC BEAMS WITH WEB OPENINGS

Luis HERRERA[1] and Anne LEMNITZER[2]

ABSTRACT

The introduction of web openings in reinforced concrete beams enables the passage of utility services and avoids low hanging ceilings that reduce effective story heights. Simultaneously it affects the overall structural behavior of the beam, the deflection profile, stress flow and hinge development. In seismically active regions beam openings have been carefully avoided given the little information and test data available in the literature. Large scale experimental studies on reinforced concrete special moment frame beams with web openings were conducted to gain insight on the cyclic response. Two reinforced concrete beams at 4/5 scale were constructed and subjected to vertical reverse cyclic loading up to 5.4% drift. Test variables include the length of the beam, arrangement of reinforcement and presence of an opening.

INTRODUCTION

The use of openings in reinforced concrete beams is a common practice in non-seismic regions and allows for passage of service lines such as water supply, electricity, air conditioning, sewage, and other mechanical services. Additionally, it prevents the creation of ceiling dead space and enables larger story heights, compact designs, and economical savings. Simultaneously, the introduction of openings modifies the structural response of a beam and creates a source of weakness in form of discontinuities in the normal flow of stresses.

A moderate amount of research work has been conducted on reinforced concrete beams with openings and primarily focused on the opening size, location, shape, and the manner in which the beam is loaded. Mansur and Tan (1999) suggested that the classification of an opening should depend entirely on the structural response of the beam. An opening can be considered "small" when the beam is able to maintain the beam type behavior and corresponding beam theories apply. When the beam type behavior ceases to exist, the opening should be classified as "large". Somes and Corley (1974) conducted testing on 19 beam specimens with varying size, location, and quantity of openings. The beams were tested under monotonic loading where strains and deflections were measured. Their study concluded that circular openings may be considered large when opening diameters exceed $0.25d_b$, where d_b is defined as the depth of the beam.

[1]Graduate Student Researcher, University of California Irvine, Irvine USA, lherrera@uci.edu
[2]Professor, University of California Irvine, Irvine USA, alemnitz@uci.edu

Other researchers such as Mansur *et al.* (1984) outlined a method to determine the collapse load of RC beams with large openings. The method applies to simply supported beams subjected to a point load at a solid section a certain distance from the end support. Beam failure is defined when a distribution of internal reaction is found such that loss of equilibrium, yield and multiple plastic hinge formation is achieved simultaneously. Tan and Mansur (1996) updated previous recommendations and proposed a step by step procedure to design RC beams with a large openings and guide the engineer in determining acceptable sizes and locations for the web openings.

Current code recommendations such as the American Concrete Institute (ACI) code does not provide straight forward design procedures for beams with openings. Section 11.1.1.1 notes that the shear strength in opening regions is significantly reduced. The commentary to this section (ACI Committee 426, Section 4.7) discusses work conducted by Lorentsen(1962) and Nasser *et al* (1967). Lorentsen (1962) tested four T-shaped beams with rectangular openings located at mid-span and concluded that openings in beams should be avoided near inflection points and additional stirrups are necessary around both sides of the opening. Nasser *et al.* conducted a series of tests on rectangular beams with large openings. In this study, the behaviors of the opening chords were found to be similar to a Vierendeel panel. When sufficient stirrups are supplied, the amount of external shear carried in each chord is proportional to their cross sectional area.

Based on the available literature, very limited research has been executed on the cyclic performance of Special Moment Frame (SMF) beams containing openings. As presented previously, the vast majority of the research focused on simply supported beams with openings of various sizes, loaded monotonically under point loads. No cyclic response data are currently published.

With the objective of gaining insight into the cyclic response, hinge development, cyclic degradation and performance of the opening region of RC beams in Special Moment Resisting Frames (SMRF), an extensive experiment testing program is currently underway at the Structural Engineering Testing Hall (SETH) Laboratory at the University of CA, Irvine. Two out of six beam experiments will be presented in this paper. The beams are replica of typical SMRF beams located in an existing structure designed per ACI 318-95 & UCB 97 recommendations. Beams were constructed as half specimens (50% of the original length) as shown in Fig. 1. Other dimensions and structural reinforcement are scaled at 80%. Reverse cyclic vertical loading was applied at the beam tip. The reinforcement of the two specimens varied slightly. Comparison of a beam with and without an opening are presented hereafter. Heavy instrumentation via internal and external sensors such as strain gauges, Linear Variable Differential Transducers (LVDTs), and String Potentiometers enabled insight into the beams rotation, overall load displacements as well as shear and flexural interaction.

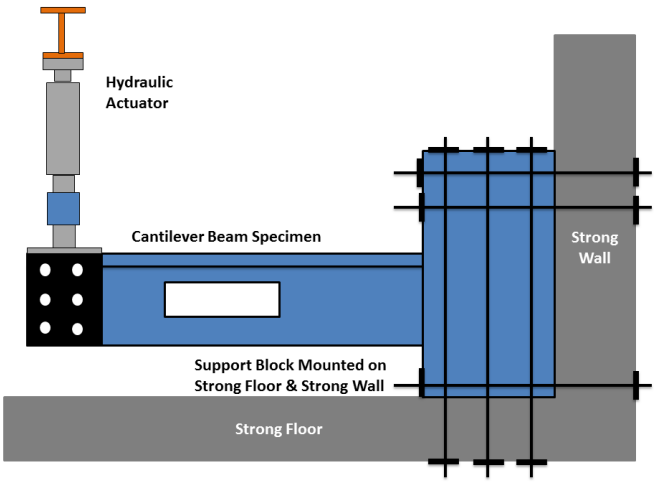

Figure 1. Test setup of ½ beam in the laboratory.

EXPERIMENTAL PROGRAM

Details of Test Specimens

Figure 2 shows the layout of test specimens 1 and 2. Specimen 1 (with opening, dark shaded in Fig. 2) has a total length of 4.01 m, a width of 0.61 m and a height of 0.97 m. The load application point was 340.34 cm away from the beam-reaction block interface. The top slab had a thickness of 12.2 cm and flanges that extended 48.8 cm from each side of the beam. The beam opening had a length of 97.5 cm and a height of 36.6 cm and was located 146.3 cm away from the reaction block/beam interface. Fig. 3 shows a typical cross-section applicable to both beam specimens.

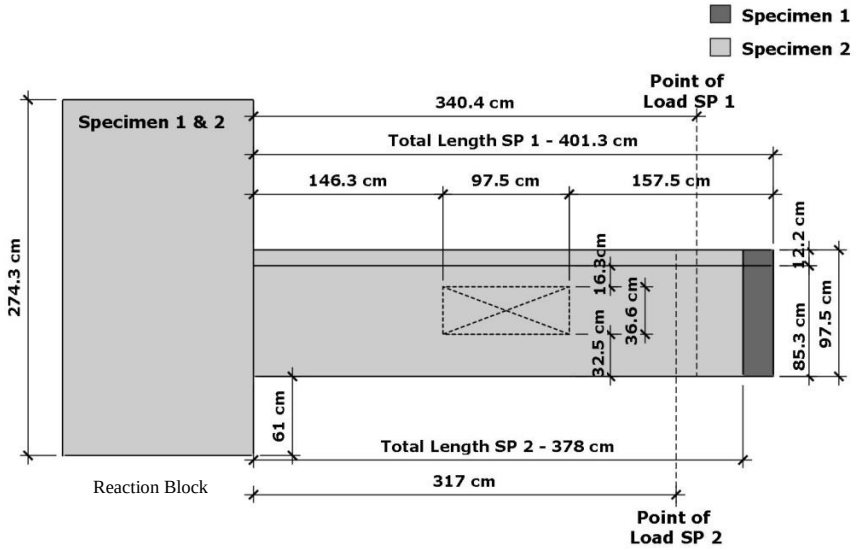

Figure 2. Schematic Layout of Specimen 1 & 2 dimensions and geometry.

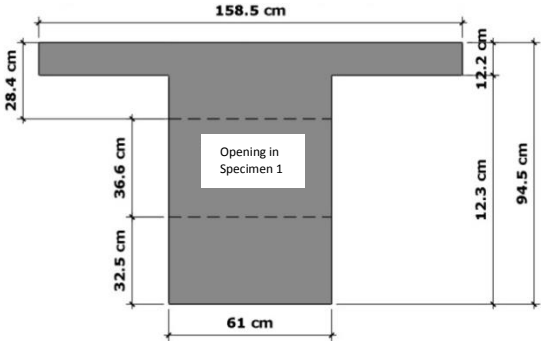

Figure 3. Typical beam cross section with dimensions (identical for both specimens).

Figs. 4 and 5 show the structural reinforcement of Specimen 1. The top longitudinal reinforcement consisted of 4#9 U bars, 2#9 and 2#7 added L bars, 4#8 and 2#7 jamb bars, and 4#9 lap bars. The bottom longitudinal reinforcement consisted of 4#9 bottom U bars, 2#9 added L bars, and an identical jamb and lap reinforcement as found at the top of the beam. The transverse reinforcement consisted of #4 stirrups with varying spacing. 4#3 side reinforcement was placed on both sides of the opening. The top flange reinforcement consisted of 4#4 longitudinal bars placed parallel to the beam and #3 bars spaced at 22.9 cm on center along the entire beam length. Table 1 explains the nominal area and diameter corresponding to each rebar size.

Table 1. Rebar Sizes

Bar Size	Diameter [mm]	Area [mm^2]
#3	9.53	71
#4	12.7	129
#7	22.2	387
#8	25.4	509
#9	28.7	645

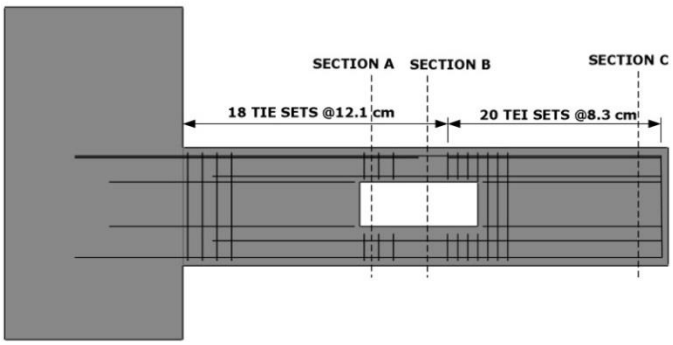

Figure 4. Side view of beam reinforcement for Specimen 1.

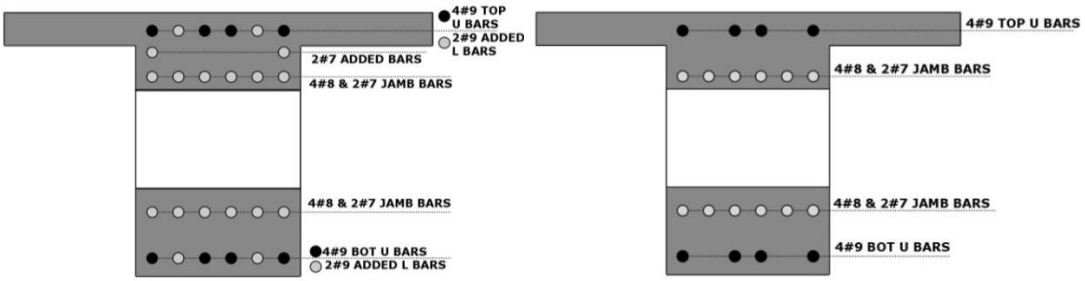

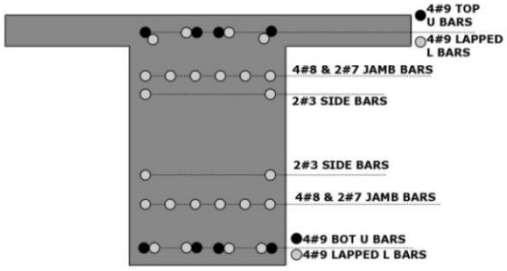

Figure 5a,b & c. Specimen 1 reinforcement at section A (top right) section B (top left) and section C (bottom).

Specimen 2 consisted of a solid cantilever beam with a length of 3.78 m. The cross section and slab dimensions are identical to Specimen 1.The load application point was 317 cm away from the face of the reaction block. Specimen 2 had bottom reinforcement of 4#8 U-shaped bars as well as 4#8 added L bars. Top reinforcement consisted of 4#9 U bars, 2#9 and 2#8 added L bars. Additionally, 4#3 bars of side reinforcement were also installed in the beam. Shear reinforcement in Specimen 2 consisted of #4 bars at varying spacing. Slab reinforcement was identical to Specimen 1. A side view of Specimen 2 reinforcement is shown in Fig. 6. Fig. 7 shows the section view of the beam at the mid and end points.

Material Properties

The concrete design mixture anticipated a minimum strength of 41.4 MPa and a slump of 12 – 15 cm to allow for easy filling below the beam opening. Slump tests on site revealed actual concrete slumps between 15.7 and 17.8 cm for all specimens. No air voids were observed after formwork removal and confirmed a proper concrete placement. The average compressive strength at the day of testing measured 53.1 and 48.3 MPa for Specimen 1 and 2 respectively. The E-moduli were back calculated for both specimens and resulted into 23449.1 MPa for Specimen 1 and 21394.4 MPa for Specimen 2. Grade 60 or Grade 60/A706 rebar was tested and reached an average yield strength of about 455.1 MPa and an

average ultimate tensile strength of about 737.7 MPa. Additional rebar testing was performed on one sample of each rebar size present in the specimen's beam through UCI and Twining Laboratories. The test results are summarized in Table 2.

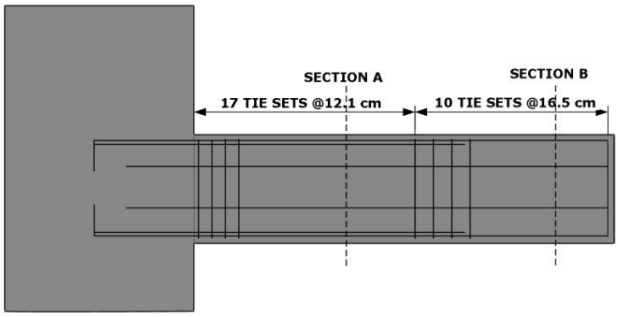

Figure 6. Side view of beam reinforcement for Specimen 2.

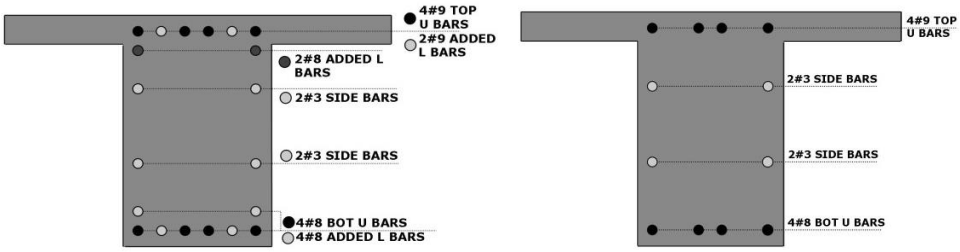

Figure 7a&b. Specimen 2 reinforcement at section A (left) Specimen 2 reinforcement at section B (right)

Table 2. Strength of Reinforcing Steel

Rebar #	Testing Lab	Yield Strength [ksi]	Yield Strength [MPa]	Ultimate Tensile [ksi]	Ultimate Tensile [Mpa]
3	UCI	65.4/65.6	450.9/452.3	98.55/95.5	679.5/658.4
4	Twining Lab	69.6	479.9	108	744.6
7	Twining Lab	66.7	459.9	108.3	746.7
8	Twining Lab	66.5	458.5	110.3	760.5
9	Twining Lab	64.3	443.3	105.94	730.4

Test Set Up: Construction

All cantilever beams were anchored in a reaction block with dimensions of approximately 2.7m in height, 1.8m in width and 1.5m in thickness. The reaction block was custom-designed for each test specimen to accommodate the force and moment requirements of the beam end reactions. The reaction block was anchored in the strong wall and strong floor via 12 high-strength dywidag bars (six in each direction) with diameters of 41.9 cm posttensioned to 48.3 MPa. The reaction block was simultaneously constructed along with the cantilever sections, since dense reinforcement spacing required a staggered erection procedure. The formwork was constructed using high strength plywood, supported by wood bracings and cross beams as shown in Fig 8a.

Concrete placement was conducted in 2 stages to create a construction joint between the beam and the top slab. Concrete placement at day 1 consisted of pouring the bottom of the reaction blocks and the beams up to a height of 5.1 cm below the beam-slab-interface.

Figure 8 a&b. Completed formwork (left) and test set up (right).

The formwork was removed approximately 7-10 days after concrete placement. The beam specimens were painted with 2 layers of white paint to enhance the visibility of crack development during testing. Additionally, a 15 x 15 cm grid was applied to each specimen to ease the identification of crack lengths and locations. Fig. 8 shows the beam with completed formwork (Fig. 8a) and after concrete pouring and formwork removal (Fig. 8b). Similarly, a U-plate system (Fig. 8b) for the vertical load application mechanism was installed and posttensioned to enable a uniform load distribution along the beam cross section and to simulate a similar curvature distribution as found in a SMF beam (i.e. close to zero rotation at the beam center). Last steps of specimen construction consisted of the installation of the external instrumentation and the setup of the data acquisition system.

Test Setup: Instrumentation

A total of 71 (Specimen1) to 52 (Specimen 2) internal and external sensors were installed on the test specimens to monitor beam displacements, rotations and internal strains during testing. The instrumentation consisted of 120 ohm Strain Gauges, LVDTs with gauge lengths ranging between +/- 2.5 and 7.6 cm and String Potentiometers with a displacement range of +/- 31.7 cm. All LVDTs were placed in plastic housing and combined with wooden extension rods to allow a larger span width as well as a protection from concrete spalling and cracking along the beam (Fig. 9). LVDTs were installed in longitudinal and diagonal configurations on both sides of the beam to measure flexural and shear deformations respectively. The string potentiometers installed on the reaction block (below and above the beam) were used to monitor and measure eventual reaction block rotations. No rotation was observed during any test. The remaining string potentiometers were installed below the beam and attached to the strong floor. Those potentiometers yielded the beam deflection curves.

Figure 9. Close up of LVDT housing and extension.

Specimen 1´s instrumentation consisted of 36 strain gauges, 28 LVDTs in longitudinal and diagonal placement and 7 string potentiometers below the beam and along the reaction block. Specimen 2´s instrumentation consisted of 20 strain gauges, 24 LVDTs in longitudinal and diagonal placement and 8 string potentiometers below the beam and along the reaction block. A schematic of external sensor location is shown in Fig. 10.

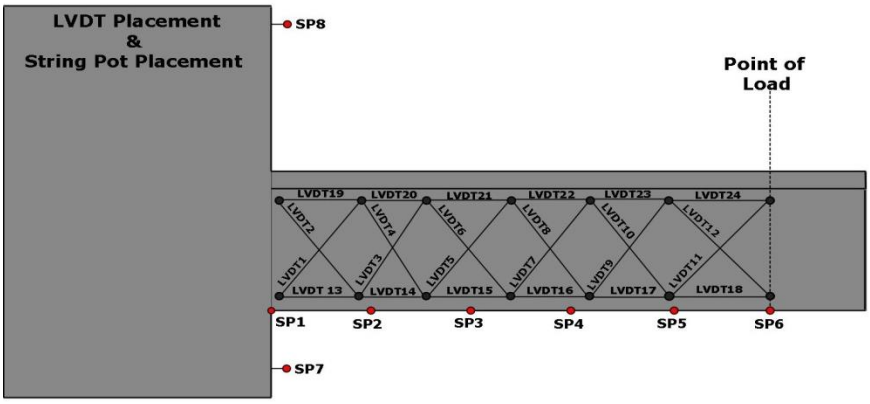

Figure 10. Typical schematic of LVDTs on face of beam and typical placement of string pots under beam and on reaction block.

TEST RESULTS

Mode of Failure

Specimen 1 showed an early crack development around the opening which then led to the development of the plastic hinge at the opening section. First observed cracks formed diagonally away from the corners of the opening. With increasing displacement levels, significant flexural cracking occurred along the bottom chord of the opening, leading to significant concrete spalling and strength degradation around the opening section. Only very minor cracking was observed at the beam/column interface. The top slab experienced significant cracks along its entire width at the location of the opening and separated from the beam during the bending cycles. Fig.11 presents the beam opening section at complete failure (4.5% drift). Excessive concrete spalling, and rebar buckling is visible in the photograph and the opening section was no longer able to transfer any applied loading in to the reaction block.

Photographs of Specimen 2 (no opening) during testing and upon test completion are shown in Fig. 12. Specimen 2 formed a plastic hinge and failed at the beam/column interface. Large diagonal cracks formed over the entire beam depth during testing. Fig.12 shows an almost parallel pattern of cracks across the beam section. Crack widths along the beam were very small (< 1 mm), cracks near the beam end opened up to widths of 2.5-5.1 cm before concrete spalling occurred and bigger pieces detached from the specimen. Significant buckling was observed in the bottom rebar of the beam as well as in the top slab reinforcement. The top slab detached from the beam after the plastic hinge formed and showed significant cracking along its entire width. However, in general the top slab added a significant amount of stiffness and capacity to the specimen and increased its capacity for the uplift cycles by approximately 40% on average.

Figure 11a&b. Deformation of Specimen 1 during a downward cycle (11a). Close up of opening after test completion (11b).

Figure 12a&b. Specimen 2: Cracks during testing (12a) and at failure (plastic hinge at beam/block interface 12b)

Load - Displacement & Moment - Rotation Relationships

Figs.13a & b display the load versus displacement and moment versus rotation relationship of Specimen 1. No self-weights of the beam and flange are considered in this plot. A positive force in Fig.13 indicates a downward push of the specimen by the actuator, hereafter referred to as compression cycle. Vice versa, when the actuator pulled up on the beam the bottom of the beam was in tension and is hereafter referred to as upward tensions cycle. The tension (upward) cycles tended to show a slightly greater force due to the additional stiffness provided by the top slab (only visible in the in the pre-yielding cycles), thereafter, the load on both cycles tend to be similarly distributed. The yield force for Specimen 1 in compression was approximately 565.5 kN at a vertical displacement of 3.2 cm (0.93% drift). Yield in tension was reached at a force of 541.8 kN at a vertical tip displacement of 2.8 cm (0.82% drift). Specimen 1 reached a maximum capacity of 653.9 kN in compression at a displacement of 6.8 cm (2.14 % drift) and about 587.2 kN in tension at a displacement of 6.9 cm (2.17 % drift). The maximum displacement of Specimen 1 was 185.4 mm in tension, corresponding to a total drift of 5.5%. The failure mode experienced by Specimen 1 was very similar to the failure modes described by Nasser *et al*(1967) and Mansur(2006). High stress concentrations around the corners of the opening lead to the initiation of diagonal cracking. Furthermore, at high displacement levels the chord members displayed a behavior similar to a Vierendeel panel including the development of plastic hinges at each corner of the opening. Overall the failure

occurred in a ductile manner where at the 3% drift ratio the diagonal cracks at the opening widened, severe spalling occurred, and the top slab separated from the beam at the location of the construction joint.

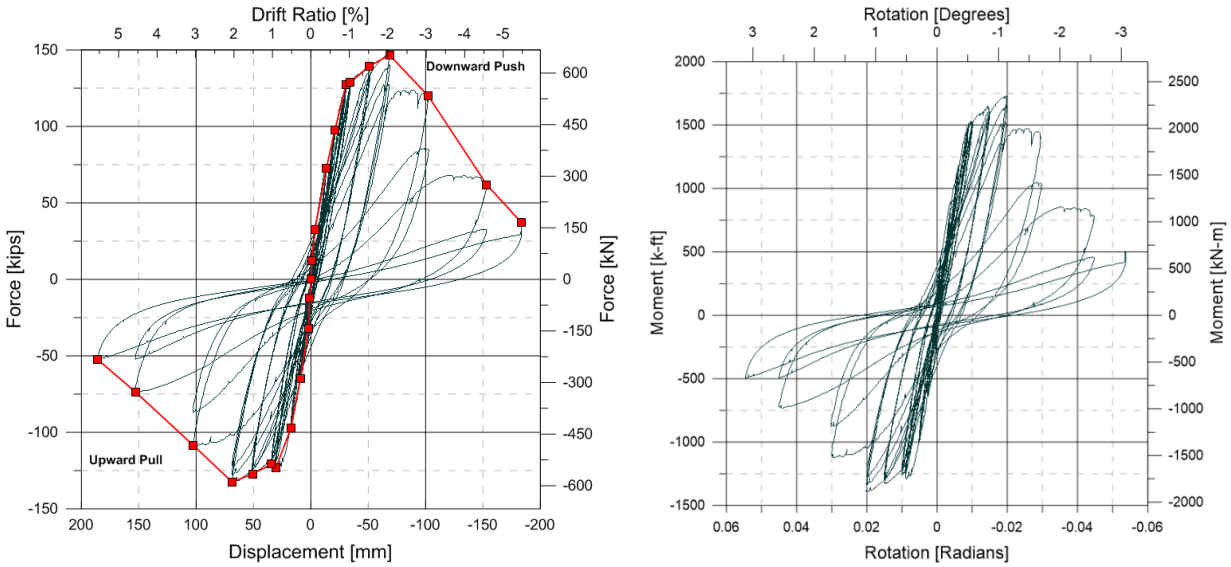

Figure 13 a&b. Force-displacement (13a) plot with back bone curve for Specimen 1(with opening) and moment-rotation plot (13b).

Table 3. Comparison of theoretical moment against measured moment.

	Level	M_{analy} kN-m (k-ft) Comp.	M_{meas} kN-m (k-ft) Comp.	M_{analy} kN-m (k-ft) Ten.	M_{meas} kN-m (k-ft) Ten.
Specimen 1	Yield	1777 (1311)	1924 (1419)	1844 (1360)	1844 (1360)
	Ultimate	1910 (1409)	2226 (1642)	1952 (1440)	1998 (1474)
Specimen 2	Yield	1707 (1259)	2123 (1566)	1504 (1109)	2081 (1535)
	Ultimate	1834 (1353)	2426 (1789)	1585 (1169)	2355 (1737)

Fig. 14 shows the load-displacement and moment-rotation relationship for Specimen 2. A testing protocol similar to the protocol developed for Specimen 1 was followed to enable general comparisons in force and displacement. The yield force for Specimen 2 in compression was approximately 669.9 kN at a vertical displacement of 3.7 cm (1.17% drift). Yield in tension was reached at a force of 656.5 kN at a vertical tip displacement of 2.9 cm (0.91% drift). Specimen 2 reached the maximum capacity of 765.1 kN in compression and 742.9 kN in tension at displacement levels of 9.6 and 9.5 cm (3.0% drift) respectively. The maximum displacement of Specimen 2 was 14.3 and 14.6 mm (4.5 and 4.6 % drift). Table 3 above presents a comparison between the measured moment and the calculated moments for both yielding and ultimate conditions. The expected values were calculated analytical studies using moment curvature analysis. Values for Specimen 1 show a general agreement whereas for Specimen 2 there is a fair amount of a deviation from the measured result, especially in the ultimate moment condition. Model calibration and subsequent analytical studies are in the future scope of this research. Overall, the measured moment values tended to be larger than those based on theory calculations.

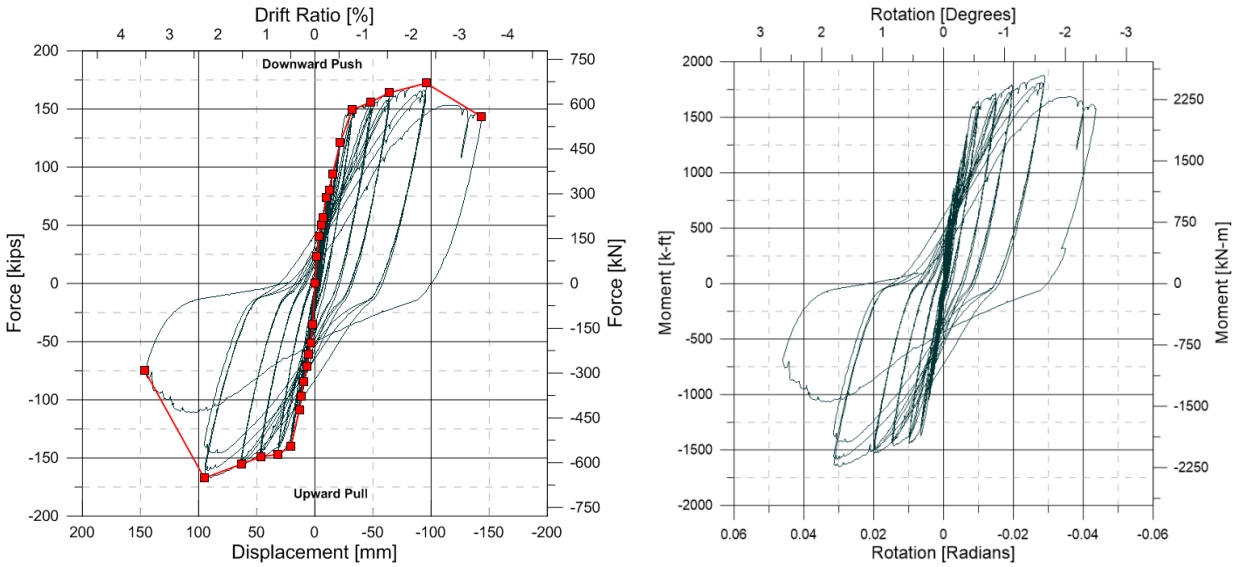

Figure 14. Force-displacement (14a) and moment-rotation (14b) plots with back bone curve for Specimen 2.

CONCLUSIONS AND FUTURE WORK

Two reinforced concrete beams scaled to 80% were tested in the SETH Lab at UC Irvine to complete structural failure. The beams are replica from an existing building and were constructed with a web opening (Specimen 1) and no web opening (Specimen 2). While general geometric properties are identical between the specimens, longitudinal and shear reinforcement varied slightly in accordance to the "as-built" state.

As expected, Specimen 1 suffered significant loss in stiffness and strength due to early cracking around the opening region. Strength loss was significant at approximately 2% drift. Specimen 1 had comparable ultimate capacities to that of Specimen 2 (no opening) with only 15% decrease in compression and a 21% decrease in tension capacity. Specimen 2 failed due to the formation of a plastic hinge at the beam-block interface. Rotation became significant after yielding in Specimen 1, while rotation was driven by the displacement of the opening region.

Four more beam specimens with different reinforcement ratios and opening locations will be constructed and tested to further study the cyclic performance of SMF beams with openings. Retrofit schemes will be investigated to strengthen the opening region. Extensive analytical studies are currently underway that investigate the effects of bottom bar buckling, slab stiffening, shear distribution and shear-flexure interaction, the application of strut and tie formulations and effect of confinement around the openings. Numerical analysis are conducted with Perform 3D, OpenSees and custom-coded Matlab procedures.

ACKNOWLEDGEMENTS

The work presented in this paper was supported by funding from Grant No. 130726.The assistance of Dr. A. Salamanca, Senior Development Engineer S. Keowen, former SETH Laboratory Manager Dr. R. Miraj and all undergraduate laboratory assistants is greatly appreciated. Kyle Monza from National Instruments and Bob Edgar from MTS are acknowledged for their continuous support with the control and data acquisition system.

REFERENCES

ACI Committee, American Concrete Institute, and International Organization for Standardization. "Building Code Requirements for Structural Concrete (ACI 318-11) and Commentary." American Concrete Institute, 2011.

Joint ACI-ASCE Committee 426, “Shear Strength of Reinforced Concrete Members (ACI 426R-74),” *Proceedings*, ASCE, V.99, No. ST6, June 1973, pp.276-288.

Lorentsen, Mogens. "Holes in reinforced concrete girders." *Informal Report, Portland Cement Association, Chicago* (1962).

Mansur, M. A., and K.H. Tan. Concrete beams with openings: analysis and design. Vol. 20. CRC Press, 1999.

Mansur, M. A., K.H. Tan, and S.L. Lee. "Collapse loads of R/C beams with large openings." *Journal of Structural Engineering* 110.11 (1984): 2602-2618.

Mansur, M. A. "Design of reinforced concrete beams with web openings." (2006): 1-17.

Nasser, Karim W., Alexander Acavalos, and H. R. Daniel. "Behavior and design of large openings in reinforced concrete beams." *ACI Journal Proceedings*. Vol. 64. No. 1. ACI, 1967.

Somes, N. F., and W. G. Corley. "Circular openings in webs of continuous beams." *ACI Special Publication* 42 (1974).

Tan, Kiang-Hwee, and Mohammad A. Mansur. "Design procedure for reinforced concrete beams with large web openings." *ACI structural journal* 93.4 (1996).